Deblurring Text Images Using Kernel Dictionaries

Tolga Dizdarer and Mustafa Ç. Pınar

***Abstract*—Image deblurring is one of the widely studied and challenging problems in image recovery. We propose a new approach to represent and compute a blurring kernel, and provide a novel method to recover text images affected by multiple kernels. We utilize some unique kernel structures to attack problems where these kernels can be estimated using linearly weighted combinations. By exploiting these structures, we provide fast and accurate solutions when dealing with certain kernel types. We demonstrate the usefulness of this methodology through computational study.**

***Index Terms*—Deblurring, text restoration, inverse problems, regularization, iterative methods**

I. Introduction

Image recovery, in general terms, deals with restoration of images in various settings whether it be corruption by noise, linear transformation, or partial loss of information. It is a widely studied problem, drawing attention from multiple disciplines. In this paper, we focus on the deblurring problem where an image that is both linearly transformed by a blur kernel and disturbed by random noise is recovered.

In general, the literature dealing with image deblurring is divided into two interconnecting settings. The first one deals with the non-blind problem, where the corrupted image is restored using a known blurring kernel. The second type is the blind case, which does not assume any knowledge of the blurring kernel and tries to estimate the blurring kernel and/or the true image. In order to overcome the limitations of each side, we design a hybrid setting where we assume a limited knowledge regarding the blurring kernel. In our model, we assume the knowledge of a dictionary of kernels, D, which consists of different types of blurring kernels $k_i \in D$ where $i = 1, ..., |D| = n$. We assume that the true kernel has a mixed distribution, which is constructed using a linear combination of kernels in D with respective weights w_i where $i = 1, ..., n$.

Our paper brings a novel perspective on how a dictionary can be constructed and utilized to deblur an image with limited information. As the model uses a limited prior knowledge, our problem lies at the intersection of blind and non-blind deblurring problems, which may be called a semi-blind deblurring. This allows us to simplify our problem both in size and complexity, leading to potential performance improvements in kernel identification. Furthermore, as we provide a new dictionary structure, our definition allows us to extend the use of our model to the completely blind deblurring problems. In that sense, we provide an argument on how the dictionaries can be utilized under different settings.

T. Dizdarer is with the Department of Operations, Information and Decisions, Wharton School, University of Pennsylvania, Philadelphia, Pennsylvania, 19104, USA (email: dizdarer@wharton.upenn.edu)

M. Ç. Pınar is with the Department of Industrial Engineering, Bilkent University, Ankara, 06800, Turkey (email: mustafap@bilkent.edu.tr)

978-1-7281-3975-3/19/$31.00 ©2019 IEEE

II. Literature Review

Various methods have been proposed to solve the image deblurring problem. Especially, with the recent advances in computing power and the deblurring problems finding applications in many recognition tasks, lately, there has been increasing rate of interest towards this problem. Many breakthrough advances have been made since the first applications on the blind deblurring such as [1], [2].

Various variational methods have been proposed to attack the image deblurring problem. These methods generally rely on regularization terms to overcome the ill-posed nature of the problem. One of the most commonly used term is the Tikhonov-Miller prior [3], which leads to solutions with small $l2$ norms. Another very commonly used prior is the edge emphasizing Total Variation term [4], which minimizes the $l1$ distance of image gradients, providing solutions with sparse edges. As sparsity of the edges is ideally represented using $l0$ minimization, many methods propose methods that penalize edge sparsity. Xu *et al*. [5] propose an unnatural $l0$ regularization term, a piece-wise function that behaves similar to $l0$ norm. Krishnan *et al*. [6] note the computational complexity of estimating $l0$ prior and proposes a normalized $l1$ prior. The prior scales the $l1$ length of the edges with $l2$ norm.

As the deblurring algorithms are very problem specific, there are methods in the literature that deal specifically with text images. Cho *et al*. [7] notice that many priors used for natural images are too weak to constrain text images. Pan *et al*. [8] use priors that enforce sparsity of the edges with another term that enforces sparsity of pixel intensities. Cao *et al*. [9] propose a method that restores text images in natural scenes using a text specific dictionary.

Some literature deal specifically with two-tone text images. Li *et al*. [10] propose a method that can jointly determine the blurring kernel and the true image. Jiang *et al*. [11] propose a two-phase method for text deblurring. First, they employ a two-tone prior to find an initial kernel estimate. In the second stage, they utilize the estimated kernel with a softer constraint on pixel intensities to estimate images that can extend beyond two-tone. Köhler *et al*. [12] propose a binarization driven text deblurring method for text images. They use a probability map that separates the background and text using a binary variable.

III. Semi-Blind Deblurring Model for Almost Binary Images

Focusing on restoration of text images, our aim is to build a method that can successfully restore image details and provide a text-like solution.

In our model we restrict our efforts to almost binary image. Almost binary, in this context, means that the pixel intensities of the image are accumulated around the extreme intensity values. Images typically have their intensities in the interval of $[0, 255]$. For our definition, we scale these values and use an intensity interval of $[0, 1]$ throughout our approach.

In our model, we denote the true image by x, blurry/noisy image by y, and the known blurring kernel by h. We assume that the true blurring kernel is a linear combination of a set of kernels in the dictionary and formulate the true image as: $y = x \circledast (\sum_{i=1}^{n} w_i h_i) + \epsilon$, where w_i is the weight of each convolution matrix in the real blurring operation.

Our formulation for the semi-blind deblurring problem is:

$$\begin{aligned} \min_{x,w} ||x \circledast (\sum_{i=1}^{n} w_i h_i) - y||^2 + \mu||\nabla x - u||^2 + \phi\Phi_0 + \lambda\Phi_1 + \gamma\Phi_2 \\ + \eta\Phi_3 + \tau||w||^2 + \theta||w||_0 \\ \text{s.t } \mathbb{1}^T w = 1 \\ ||w||_0 \leq \Gamma \\ w \geq 0. \end{aligned} \tag{1}$$

where Φ_0 denotes the convex regularization terms and $\Phi_i, i = 1, 2, 3$ denote separate non-convex regularization terms. These terms are explicitly:

$$\begin{aligned} \Phi_0 = ||\nabla_v x \circledast h - \nabla_v y||^2 + ||\nabla_h x \circledast h - \nabla_h y||^2 \\ + \frac{\nu}{\phi}(||\nabla_{hh} x||^2 + ||\nabla_{vv} x||^2), \end{aligned} \tag{2}$$

$$\Phi_1 = ||\nabla x||_0, \tag{3}$$

$$\Phi_2 = ||x||_0 + \frac{\zeta}{\gamma}||1 - x||_0, \tag{4}$$

$$\Phi_3 = -(||x||^2 + ||1 - x||^2). \tag{5}$$

The main term in the objective function minimizes the $l2$ difference between the observed image and blurred image. It is known that minimizing $l2$ length of the noise is especially effective at treating Gaussian noise, which is used in many applications as expressed in [13].

The convex regularization term, Φ_0, utilizes two different ideas. First part of the term uses first derivative in horizontal and vertical directions to minimize the difference between blurred and observed edges. Second part of the term minimizes the second derivative of the image. This term pushes the model to provide images with derivatives that are persistent in horizontal and/or vertical directions.

The remaining terms are non-convex. Φ_1, minimizes the number of non-zero edges. As the almost binary text images generally have pixels that have neighboring pixels with similar intensities, the resulting image is expected to have a small number of non-zero edges. Although this element is non-convex, [8] proposes a method to estimate a local solution for an optimization problem with this regularizer. Φ_2 minimizes the number of pixels that do not have intensities of 0 or 1. Φ_3 is a concave term. As this expression is smooth and decreasing towards both edges, it favors solutions closer to extreme pixels, 0 and 1. We use this expression to shift the non-extreme values to edges, which iterates a current solution towards an almost binary image.

As we approach deblurring through a dictionary of kernels, which can be large in size, solving for w may result in a kernel that over-fits the corresponding blurred image y. In other words, the model may disregard the effect of noise in the image by attaching positive weights to kernels that have zero weight in the true kernel, due to its motivation to reduce the objective. In an effort to overcome this problem, we use a method similar to [14] and put a restriction on the sparsity of kernel elements through the last two regularization terms.

Following the general approach in the literature, we tackle the problem by solving for x and w successively. This decomposition of the problems leads to the following two subproblems:

$$\begin{aligned} \min_{x} ||x \circledast (\sum_{i=1}^{n} w_i h_i) - y||^2 + \mu||\nabla x - u||^2 + \lambda\Phi_1 + \phi\Phi_0 + \gamma\Phi_2 \\ + \eta\Phi_3, \end{aligned} \tag{6}$$

$$\begin{aligned} \min_{w} ||x \circledast (\sum_{i=1}^{n} w_i h_i) - y||^2 + \tau||w||^2 + \theta||w||_0 \\ \text{s.t } \mathbb{1}^T w = 1 \\ ||w||_0 \leq \Gamma \\ w \geq 0. \end{aligned} \tag{7}$$

We explore the solutions to problems 6 and 7 in Sections III-A and III-B respectively.

A. Image Restoration Subproblem

The subproblem has three non-convex regularization terms, which can lead to an ill-defined problem structure. As a result, we restrict our attention to finding a local solution for this problem. First, we use the alternating minimization method proposed in [8] to overcome the non-convexity induced by the first regularization term, Φ_1. Then, the problem reduces to the following two models, which we will solve alternatingly:

$$\min_{x} ||x \circledast H - y||^2 + \mu||\nabla x - u||^2 + \phi\Phi_0 + \gamma\Phi_2 + \eta\Phi_3 \tag{8}$$

where $H = \sum_{i \in D} w_i h_i$ and

$$\min_{u} \lambda||u||_0 + \mu||\nabla x - u||^2. \tag{9}$$

We can solve eq. (9) by simple algebra. Its solution is:

$$u_i^* = \begin{cases} \nabla x_i & , (\nabla x_i)^2 \geq \frac{\lambda}{\mu} \\ 0 & ,\text{otherwise.} \end{cases} \tag{10}$$

In order to solve eq. (8), we need a method that can reliably find local solutions for large-scale, non-convex problems. In our computational study, we use the Accelerated Inexact Proximal Gradient proposed in [15]. First, we split our objective function terms into convex and non-convex parts. We denote

our convex elements by function f and non-convex elements by function g:

$$f(x) = ||x \circledast H - y||^2 + \mu||\nabla x - u||^2 + \phi(||\nabla_v x \circledast H - \nabla_v y||^2 + ||\nabla_h x \circledast H - \nabla_h y||^2) + \nu(||\nabla_{hh} x||^2 + ||\nabla_{vv} x||^2), \tag{11}$$

and

$$g(x) = \gamma||x||_0 + \zeta||1 - x||_0 - \eta(||x||^2 + ||1 - x||^2). \tag{12}$$

Using these functions, we can compute x iteratively, where each iterate x_s is found by using proximal gradient:

$$x_s = prox_{t_s}(g)(x_{s-1} - t_s \nabla f(x_{s-1})). \tag{13}$$

As f is smooth and convex, we can find its gradient. Moreover, we can compute its value very efficiently using the Fast Fourier Transform [16].

Assigning $z_s = x_{s-1} - t_s \nabla f(x_{s-1})$, we compute x_s through the following minimization problem:

$$x_s = prox_{t_s}(g)(z_s) = \underset{u}{\operatorname{argmin}}\{\gamma||u||_0 + \zeta||1 - u||_0 - \eta(||u||^2 + ||1 - u||^2) + \frac{1}{t_s}||u - z_s||^2\}. \tag{14}$$

Notice that this minimization problem is equivalent to:

$$\begin{aligned} prox_{t_s}(g)(z_s) &= \underset{u}{\operatorname{argmin}}\{\gamma \sum_{\forall i}||u_i||_0 + \zeta \sum_{\forall i}||1 - u_i||_0 \\ &\quad - \eta(\sum_{\forall i}(u_i)^2 + \sum_{\forall i}(1 - u_i)^2) + \frac{1}{t_s}\sum_{\forall i}(u_i - z_{s_i})^2\} \\ &= \sum_{\forall i} \underset{u}{\operatorname{argmin}}\{\gamma||u_i||_0 + \zeta||1 - u_i||_0 - \eta((u_i)^2 \\ &\quad + (1 - u_i)^2) + \frac{1}{t_s}(u_i - z_{s_i})^2\}. \end{aligned} \tag{15}$$

This minimization problem is separable in u_i. To search for the optimal solution for each u_i we need to consider three cases: $u_i = 0$, $u_i = 1$ and $u_i \neq \{0, 1\}$:

Case 1: If $u_i = 0$:

$$\begin{aligned} c_i^{lb} &= \gamma||u_i||_0 + \zeta||1 - u_i||_0 - \eta(u_i^2 + (1 - u_i)^2) \\ &\quad + \frac{1}{t_s}(u_i - z_{s_i})^2 \\ &= 0 + \zeta - \eta(0 + 1^2) + \frac{1}{t_s}z_{s_i}^2 \\ &\implies c_i^{lb} = \zeta + \frac{1}{t_s}z_{s_i}^2 - 1^2\eta. \end{aligned}$$

Case 2: If $u_i = 1$:

$$\begin{aligned} c_i^{ub} &= \gamma||u_i||_0 + \zeta||1 - u_i||_0 - \eta(u_i^2 + (1 - u_i)^2) \\ &\quad + \frac{1}{t_s}(u_i - z_{s_i})^2 \\ &= \gamma + 0 - \eta(1^2 + 0) + \frac{1}{t_s}(1 - z_{s_i})^2 \\ &\implies c_i^{ub} = \gamma + \frac{1}{t_s}(1 - z_{s_i})^2 - 1^2\eta. \end{aligned}$$

Case 3: If $u_i \neq \{0, 1\}$:

$$\begin{aligned} c_i^{mid} &= \gamma||u_i||_0 + \zeta||1 - u_i||_0 - \eta(u_i^2 + (1 - u_i)^2) \\ &\quad + \frac{1}{t_s}(u_i - z_{s_i})^2 \\ &= \zeta + \gamma + \min_{u_i}\{-\eta u_i^2 - \eta(u_i^2 - 2u_i + 1^2) + \frac{1}{t_s}(u_i^2 - 2u_i z_{s_i} + z_{s_i}^2)\}. \end{aligned}$$

The inner minimization problem is a polynomial of degree two. Notice that for a parameter choice, η, that satisfies $\frac{1}{t_s} - 2\eta > 0$, this problem becomes a convex minimization problem. Under this restriction, the minimum is attained at:

$$u_i = \frac{\frac{z_{s_i}}{t_s} - \eta}{\frac{1}{t_s} - 2\eta}.$$

We substitute this solution back into the inner minimization problem to find the optimal c_i^{mid}. We use the values c_i^{lb}, c_i^{ub}, c_i^{mid} to compare the cases and determine the global minimizer. We assign x_i the value of u_i that leads to the minimum objective.

$$x_i^* = \begin{cases} 0 & , c_i^{lb} < \min\{c_i^{ub}, c_i^{mid}\} \\ 1 & , c_i^{ub} < \min\{c_i^{lb}, c_i^{mid}\} \\ \frac{\frac{z_{s_i}}{t_s} - \eta}{\frac{1}{t_s} - 2\eta} & ,\text{otherwise.} \end{cases} \tag{16}$$

B. Kernel Restoration Subproblem

First, we note that the convolution operator has the distributive property [17]. Moreover, convolution operator is associative with scalar multiplication. So, we can alternatively represent the observed image as:

$$y = x \circledast (\sum_{i=1}^{n} w_i h_i) + \epsilon = \sum_{i=1}^{n} w_i (x \circledast h_i) + \epsilon. \tag{17}$$

We use this fact to be able to formulate the problem as a function of w. In order to overcome the non-convexity induced by the $l0$ term in the objective, we use the alternating minimization method [8] and solve the two following subproblems alternatingly:

$$\begin{aligned} &\min_w ||\sum_{i \in D}^{n} w_i U_i^* - y||^2 + \tau||w||^2 + \alpha||w - v||^2 \\ &\text{s.t } \mathbb{1}^T w = 1 \\ &\quad w \geq 0 \end{aligned} \tag{18}$$

where $U_i^* = x \circledast h_i$ and

$$\min_v \alpha||w - v||^2 + \theta||v||_0. \tag{19}$$

We can use simple algebra to find the optimal solution of eq. (19):

$$v_i^* = \begin{cases} w_i & , (w_i)^2 \geq \frac{\theta}{\alpha} \\ 0 & ,\text{otherwise.} \end{cases} \tag{20}$$

Moreover, for fixed U^* values, we can express eq. (18) as a QP with equality and inequality constraints and solve it using any Non-Negative Least Squares method.

After solving both subproblems we summarize our algorithm in algorithm 1 below.

Algorithm 1 Almost Binary Deblurring Algorithm

procedure SEMI-BLIND DEBLUR(y)
  Assign $s_0, \phi, \lambda, \gamma, \zeta, \eta, \mu$
  Set $x \leftarrow y$,$w \leftarrow \frac{1}{n}\begin{bmatrix}1 & 1 & ... & 1\end{bmatrix}^T$,$s \leftarrow 1$,$t \leftarrow 1$
  while $t < t_{max}$ **do**
    Set $s \leftarrow 1$
    while $s < s_{max}$ **do**
      Solve for u using eq. (10)
      Compute z_s by using the derivative of eq. (11)
      Find the proximal mapping x_s by utilizing eq. (16)
      $\mu \leftarrow 2\mu$, $s \leftarrow s + 1$
    end-while
    if s=1 **then**
      Set $v \leftarrow 0$
    else
      Solve for v using eq. (20)
    end-if
    Solve for w using NNLS Solver on eq. (18)
    Set $\theta \leftarrow 2\theta$, $t \leftarrow t + 1$
  end-while

IV. COMPUTATIONAL STUDY

Our experiments in the computational study are conducted over images that have varying sizes, ranging from 500x500 to 1000x1000 pixels. For blurring kernels, we use randomly generated kernels which are linear combinations of Motion-blur and/or Gaussian kernels All of the images are disturbed by Gaussian noise with Signal-to-Noise Ratio of 40.

To verify the effectiveness of our proposed model, we present two images constructed with different blurring kernels and random noises. We test the model under the assumption that the blurring kernel is known and compare our findings with other applications in the literature. We get the results reported in figs. 1 and 2. We also compare the PSNR and SSIM values of the estimated images. They are given in tables I and II.

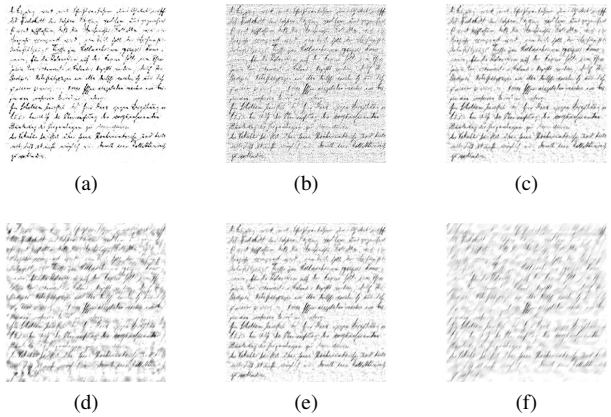

(a) (b) (c) (d) (e) (f)

Fig. 1: (a)Our method. (b)Lucy-Richardson Algorithm [18], [19]. (c)Total Variation [4]. (d)l0 regularized model [8]. (e) Hyper-laplacian priors [20]. (f) [21].

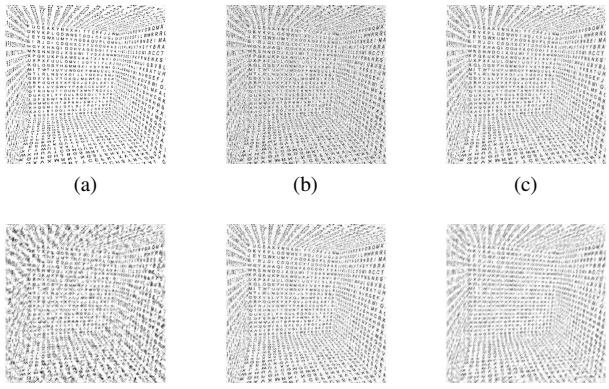

(a) (b) (c) (d) (e) (f)

Fig. 2: (a)Our method. (b)Lucy-Richardson Algorithm [18], [19]. (c)Total Variation [4]. (d)l0 regularized model [8]. (e) Hyper-laplacian priors [20]. (f) [21].

TABLE I: The comparison of PSNR values for estimated images

Image	Our Method	Lucy Richard-son [18], [19]	Total Vari-ation [4]	L0 Regu-lariza-tion [8]	Hyper Lapla-cian [20]	Outliers [21]
Vector	15.526	18.222	14.603	15.426	**19.949**	14.598
Handwriting	**18.740**	15.010	17.875	15.973	17.688	15.973
Cube	**14.545**	12.447	13.264	11.850	12.959	11.998
Cartoon	**28.457**	14.876	19.757	22.038	18.750	17.645

TABLE II: The comparison of SSIM values for estimated images

Image	Our Method	Lucy Richard-son [18], [19]	Total Vari-ation [4]	L0 Regu-lariza-tion [8]	Hyper Lapla-cian [20]	Outliers [21]
Vector	0.8776	**0.9333**	0.7337	0.7451	0.7574	0.6623
Handwriting	**0.8199**	0.5449	0.6790	0.5474	0.6688	0.4807
Cube	**0.8438**	0.7103	0.7493	0.6015	0.7204	0.5626
Cartoon	**0.9926**	0.4307	0.6324	0.7264	0.5309	0.7414

We find that, compared to some existing literature, our model performs quite favorably in terms of delivering a text-like solution. Whereas many methods are qualified to find a solution that can recover text structures, our model specializes in providing a solution that looks like a text image without noise. In order to provide a sample of the convergence characteristic of our model, we plot in Table 3 the total change in intensity and resulting PSNR values of the interim image throughout the iterations for an observation.

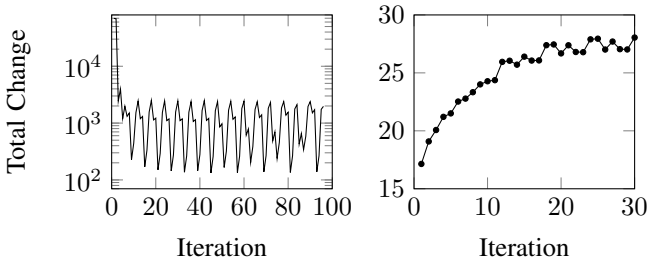

Fig. 3: Intensity change and PSNR value of the restored image through iterations.

V. Sensitivity Analysis

Generally, in deblurring models, the solutions are very sensitive to change in regularization parameters. For this reason, we also consider how our solution changes when we change our assigned parameter values. As our model is highly non-convex we analyze the sensitivity of our model to parameter weights by computing the solution for different values of $\phi, \nu, \mu, \gamma, \zeta$ and η for the Handwriting image. For each weight, we fix the other parameters and scale its value by 15 different weights ranging from 0 to 50. We compute and plot the $l2$ distance between our optimal solution and the solution with the new scale. Our findings are in fig. 5.

We find that for a small change in parameters values, the estimated solution does not show a significant change. Increasing or decreasing the parameter values by less than 15% results in a change of at most 1% at the newly estimated image. We also find that the maximum change in intensity for any pixel of the estimated images is 25 for this case. However, we find larger changes to have more extreme effects on the solution. For example, increasing the parameter values by more than 100% may lead to a change of more than 150 in intensity value fo some pixels, showing that the sensitivity gradually increases when we shift away from our assigned values.

To show the effects of individual parameters on the restored image, we compare some details in our restored images with the solution we would get if we omitted those parameters. We present the findings for a subset of the parameters in Figures 4.

VI. Specially Structured Blur Kernels

We have stated before that our representation of a blurring kernel as linear combination of simpler kernels allows us to efficiently pursue the true kernels for some specialized settings. As an example, let us consider an image that is affected by both motion and out-of-focus blurs. This blurring operation may be formulated as:

$$y = x \circledast h_{\text{motion}} \circledast h_{\text{out-of-focus}} + \epsilon. \tag{21}$$

If we were to approach this problem as a blind deblurring problem with no prior knowledge, we would consider a solution space that spans a large dictionary where each element represents one unique pixel that has a positive probability of being present in the true kernel. Although this approach is required for the blind problem, for settings where there is

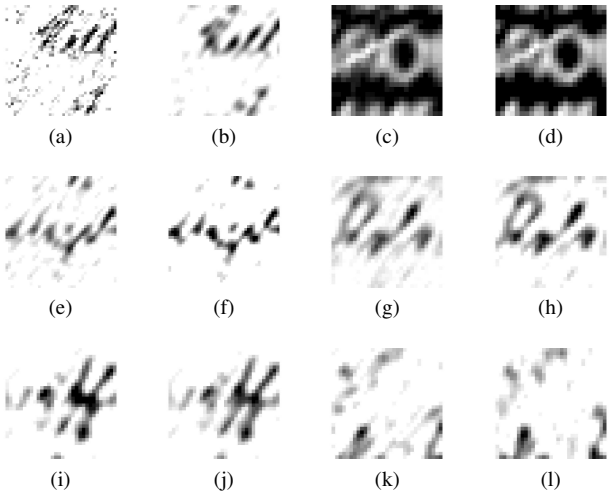

Fig. 4: Estimated solution. (a)Without ν. (b)With ν. (c)Without γ. (d)With γ. (e)Without ζ. (f)With ζ. (g)Without η. (h)With η. (i)Without μ. (j)With μ. (k)Without ϕ. (l)With ϕ.

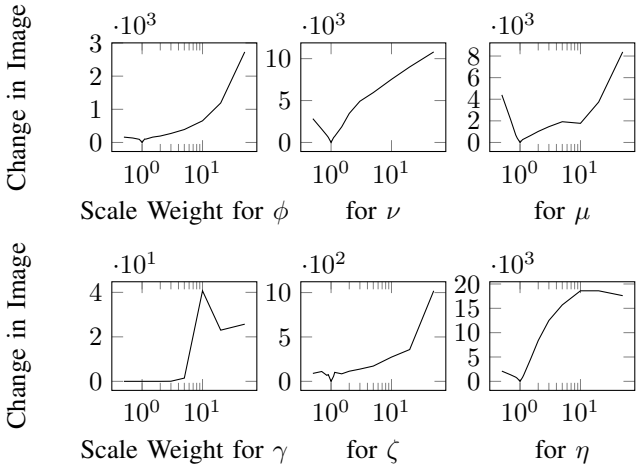

Fig. 5: Total $l2$ change in the estimated when we scale parameters.

additional information about the kernel, we propose a more efficient approach.

Let us assume that the true blur kernels have the following structures:

$$h_{\text{motion}} = \sum_{i=1}^{N} h_i^m \quad \text{and} \quad h_{\text{out-of-focus}} = \sum_{j=1}^{M} h_j^o. \tag{22}$$

where h_{motion} and $h_{\text{out-of-focus}}$ are dictionary elements constructed based upon our prior knowledge on the blurring kernels. We can use the distributive property of convolution operator to show that:

$$\begin{aligned} y =& x \circledast h_{\text{motion}} \circledast h_{\text{out-of-focus}} + \epsilon = x \circledast \sum_{i=1}^{N} h_i^m \circledast \sum_{j=1}^{M} h_j^o + \epsilon \\ =& \sum_{i=1}^{N}\sum_{j=1}^{M} x \circledast h_i^m \circledast h_j^o + \epsilon = \sum_{l=1}^{NM} x \circledast h_l^* + \epsilon, \end{aligned} \tag{23}$$

where $h_l^* = h_i^m \circledast h_j^o$ for $l = j(N-1)+i$. This fact allows us to construct a single dictionary that can represent the convolution of two unique kernel types.

As an example, assume that we are dealing with a motion and out-of-focus blurred image, where the motion blur is known to have an angle of 90^o and odd length between 9 and 13 pixels. Similarly assume that the out-of-focus is known to have an odd radius between 13 and 17. For this problem, we can construct individual dictionary sets, h_i^m and h_j^o which contain the necessary elements to build motion blur and out of focus blur respectively. In both of the sets, the elements are specially constructed partitions of the pixels necessary to construct the true kernels. Each element supplements a unique pixel group, which collectively contain the sufficient pixel groups to perfectly restore any blur kernel within the search space. After constructing the individual sets, we can compute the dictionary for convolved kernel, h_l, by computing the pairwise convolution of the elements of the two sets. As both of these sets will have 3 sub-kernels, the resulting dictionary will have only 9 elements. Comparing to the blind problem where the model will consist of finding the intensity of 289 pixels, this approach greatly reduces the size of the problem. Assuming that we solve the problem for the setting where the original motion kernel has a size of 11 and the out-of-focus kernel has a radius of 15, we recover the image and kernel provided in fig. 6.

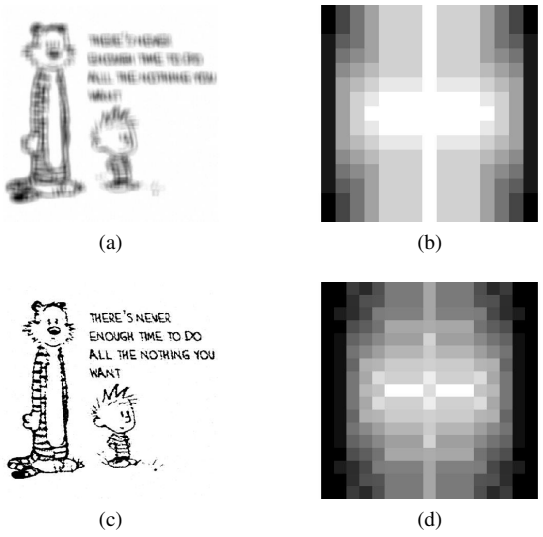

(a) (b) (c) (d)

Fig. 6: Image affected by multiple blurring kernels recovered using specially designed dictionary. (a)Observed Image. (b)True Kernel. (c)Restored Image. (d)Restored Kernel.

VII. Conclusion

In this paper, we propose a novel method for deblurring text images under blind and semi-blind settings. We provide an algorithm that can solve such problems by using efficient optimization methods. While our algorithms and computational study focused extensively on applications to almost binary images, they can be extended to various different settings in future research. One of the research directions we are interested in is to allow images to have multiple accumulation points, which would allow one to deblur images with multiple layers. Another research direction we find interesting is images with backgrounds that have a change in intensity through some direction. Modifying the model to work with such images can allow one to deal with a setting where the object of interest is not uniformly illuminated.

References

[1] T. G. Stockham, T. M. Cannon, and R. B. Ingebretsen, "Blind deconvolution through digital signal processing," *Proceedings of the IEEE*, vol. 63, no. 4, pp. 678–692, April 1975.

[2] M. Cannon, "Blind deconvolution of spatially invariant image blurs with phase," *IEEE Transactions on Acoustics, Speech, and Signal Processing*, vol. 24, no. 1, pp. 58–63, Feb 1976.

[3] A. N. Tikhonov, "Solution of incorrectly formulated problems and the regularization method," *Soviet Math. Dokl.*, vol. 4, pp. 1035–1038, 1963.

[4] L. I. Rudin, S. Osher, and E. Fatemi, "Nonlinear total variation based noise removal algorithms," *Physica D: Nonlinear Phenomena*, vol. 60, no. 1-4, pp. 259–268, 1992.

[5] L. Xu, S. Zheng, and J. Jia, "Unnatural l0 sparse representation for natural image deblurring," in *Proceedings of the IEEE conference on computer vision and pattern recognition*, 2013, pp. 1107–1114.

[6] D. Krishnan, T. Tay, and R. Fergus, "Blind deconvolution using a normalized sparsity measure," in *CVPR 2011*. IEEE, 2011, pp. 233–240.

[7] H. Cho, J. Wang, and S. Lee, "Text image deblurring using text-specific properties," in *European Conference on Computer Vision*. Springer, 2012, pp. 524–537.

[8] J. Pan, Z. Hu, Z. Su, and M.-H. Yang, "Deblurring text images via l0-regularized intensity and gradient prior," in *2014 IEEE Conference on Computer Vision and Pattern Recognition*, June 2014, pp. 2901–2908.

[9] X. Cao, W. Ren, W. Zuo, X. Guo, and H. Foroosh, "Scene text deblurring using text-specific multiscale dictionaries," *IEEE Transactions on Image Processing*, vol. 24, no. 4, pp. 1302–1314, 2015.

[10] T.-H. Li and K.-S. Lii, "A joint estimation approach for two-tone image deblurring by blind deconvolution," *IEEE Transactions on Image Processing*, vol. 11, no. 8, pp. 847–858, 2002.

[11] X. Jiang, H. Yao, and S. Zhao, "Text image deblurring via two-tone prior," *Neurocomputing*, vol. 242, pp. 1–14, 2017.

[12] T. Köhler, A. Maier, and V. Christlein, "Binarization driven blind deconvolution for document image restoration," in *German Conference on Pattern Recognition*. Springer, 2015, pp. 91–102.

[13] C. A. Micchelli, L. Shen, Y. Xu, and X. Zeng, "Proximity algorithms for image models ii: L1/tv denosing," *Advances in Computational Mathematics, online version available*, 2011.

[14] C. C. Lee and W. L. Hwang, "Sparse representation of a blur kernel for out-of-focus blind image restoration," in *2016 IEEE International Conference on Image Processing (ICIP)*, Sept 2016, pp. 2698–2702.

[15] B. Gu, Z. Huo, and H. Huang, "Inexact proximal gradient methods for non-convex and non-smooth optimization," *arXiv preprint arXiv:1612.06003*, 2016.

[16] W. H. Press, *Numerical recipes 3rd edition: The art of scientific computing*. Cambridge university press, 2007.

[17] M. H. Hayes, *Schaum's outline of digital signal processing*. McGraw-Hill, Inc., 1998.

[18] W. H. Richardson, "Bayesian-based iterative method of image restoration∗," *J. Opt. Soc. Am.*, vol. 62, no. 1, pp. 55–59, Jan 1972. [Online]. Available: http://www.osapublishing.org/abstract.cfm?URI=josa-62-1-55

[19] L. B. Lucy, "An iterative technique for the rectification of observed distributions," *The Astronomical Journal*, vol. 79, p. 745, Jun. 1974.

[20] D. Krishnan and R. Fergus, "Fast image deconvolution using hyper-laplacian priors," in *Advances in neural information processing systems*, 2009, pp. 1033–1041.

[21] S. Cho, J. Wang, and S. Lee, "Handling outliers in non-blind image deconvolution," in *Computer Vision (ICCV), 2011 IEEE International Conference on*. IEEE, 2011, pp. 495–502.